Enhancing power quality in wireless DC power supplies through active power filtering: A computer simulation approach

Rahimi Baharom, Wan Muhamad Hakimi Wan Bunyamin
Power Electronics Research Group, School of Electrical Engineering, College of Engineering, Universiti Teknologi MARA, Shah Alam, Malaysia

Article Info

ABSTRACT

This paper presents a computer simulation model for a high-power factor wireless DC power supply system, integrating an active power filter (APF) at the rectifier stage on the transmitter side using a rectifier boost technique. The APF, employing a MOSFET switch regulated by active pulse width modulation (APWM) within a current control loop, addresses pulsating and distorted AC supply currents caused by non-linear loads. A robust closed-loop control mechanism, including a subtractor circuit, proportional-integral (PI) controller, and comparator, ensures the generation of a continuous sinusoidal waveform synchronized with the supply voltage. The model utilizes a high-frequency inverter to convert DC to AC, which is then wirelessly transmitted via wireless power transfer (WPT) technology and converted back to DC by a high-frequency rectifier. MATLAB/Simulink simulation results show a significant reduction in total harmonic distortion (THD) of the AC supply current, complying with IEEE 519 standards. Selected results are presented to verify the proposed method's effectiveness in reducing harmonic distortions and enhancing power quality. This study highlights the advantages of WPT in scenarios where traditional wired connections are impractical and underscores the potential of this system for real-world applications, particularly in developing high-power factor wireless DC power supply systems.

Corresponding Author:

Rahimi Baharom
Power Electronics Research Group, School of Electrical Engineering, College of Engineering
Universiti Teknologi MARA
40450 Shah Alam, Selangor, Malaysia
Email: rahimi6579@gmail.com

1. INTRODUCTION

Power supplies are essential for delivering consistent and reliable electrical energy to a wide array of devices and systems. They are fundamentally categorized into two types: alternating current or AC and direct current or DC power supplies. DC power supplies, in particular, have become increasingly popular due to their versatility and specific benefits for modern electronics. These benefits include reduced line costs, lower transmission losses, rapid energy availability, high reliability, and increased transmission capacity compared to AC power [1]. The principal components of a DC power supply system are the transformer, rectifier, filter, and regulator [2]-[3]. Initially, the transformer reduces the incoming AC voltage to a manageable level, which is then converted to pulsing DC by the rectifier. The filter smooths these pulses, and the regulator maintains a constant output voltage. DC power supplies are widely utilized in sectors such as consumer electronics, telecommunications, industrial automation, and renewable energy systems. Typically, an AC to DC converter transforms AC power from the source into the DC power output, which can introduce distortion to the current supply, leading to a low power factor, significant harmonic content, and elevated total harmonic distortion

(THD) levels [4]. The proliferation of current harmonics is detrimental to power quality. These harmonics, sinusoidal waveforms at frequencies that are multiples of the power line frequency, can unbalance the system, escalating the THD level. Power electronic devices, representing non-linear loads, majorly contribute to current harmonics, potentially causing equipment failure, reducing efficiency, lowering the power factor, and increasing losses [4]-[6].

Addressing power quality issues can be achieved through several methods, including power factor correction, harmonic filtering, and voltage regulation. This paper concentrates on harmonic filtering via active power filters (APF), a cutting-edge solution employing power electronics to generate compensatory currents [2], [3]. APFs seamlessly integrate into power systems, neutralizing harmonic components and converting the supply current into a continuous, sinusoidal waveform in harmony with the supply voltage. This significantly improves the power factor and dramatically reduces the supply current's THD [7]-[9], leading to reduced losses, enhanced equipment reliability, and an overall betterment of the power supply system.

The transition to wired DC power supplies reveals inherent limitations in their adaptability and efficiency across various applications. Wired connections confine devices to specific locations, hindering mobility and flexibility, and contributing to a cluttered appearance while possibly introducing safety hazards. Furthermore, electromagnetic and radio frequency interference in wired systems can compromise reliability. These challenges are surmountable through the adoption of wireless power transfer (WPT) in DC power supply systems.

WPT technologies facilitate the transmission of electrical energy without the need for cables or wires [10]-[12], garnering significant interest as an alternative to traditional cable-based power transfer methods. Applicable to a broad spectrum of devices, including cell phones, computers, TVs, and electric vehicles [13]-[15], WPT enhances device mobility and flexibility [16]. Utilizing transmitter and receiver coils driven by a high-frequency AC inverter, WPT accomplishes the wireless transmission of power [17]. These inverters are pivotal in converting DC to high-frequency AC, crucial for effective WPT [18], with the necessity for high frequency stemming from its reliance on magnetic field coupling to transmit energy wirelessly [19]-[21]. The increased switching frequency of the high-frequency inverters enhances the generation of a magnetic field, thereby facilitating efficient energy transfer. The AC received by the receiver coil is subsequently converted back into DC power via a high-frequency rectifier. In this process, a set of four diodes is utilized, effectively switching to manage both the positive and negative half-cycles. This precise synchronization ensures a smooth and continuous DC output, enhancing the overall efficiency and reliability of the power conversion [22]-[25].

This paper addresses the challenges of wired DC power supplies by developing a wireless system that improves mobility, compatibility, and safety. The proposed wireless DC power supply emphasizes user convenience and aims to enhance power supply flexibility. Additionally, the project focuses on reducing power factor and efficiency losses due to harmonic currents from non-linear loads. By incorporating an APF with WPT technology, the system minimizes THD in the supply current to comply with IEEE 519 standards [26], improving power factor and overall efficiency. This approach enhances system performance and sets new standards for power quality in wireless DC power transfers.

2. THE PROPOSED WIRELESS DC POWER SUPPLY SYSTEM

Figure 1 provides a comprehensive block diagram of a high power factor wireless DC power supply system, illustrating the sequence of stages involved in converting and transmitting power from an AC source to a DC load wirelessly. Each block in the diagram represents a crucial component or process that contributes to the overall functionality and efficiency of the system. The process begins with the AC Supply, which is the initial source of power. The AC provided by this supply is typically characterized by harmonic distortions that can negatively impact power quality. To address this, the system incorporates APF. The APF is designed to reduce harmonic distortions and improve the power factor by filtering out unwanted harmonics from the AC supply, ensuring that the subsequent stages receive a cleaner and more stable current.

Following the filtration, the AC to DC rectification (single-phase rectifier circuit) stage converts the filtered AC into DC. This rectification process involves a single-phase rectifier circuit that changes the AC input to a pulsing DC output. The conversion is crucial for the next stage, where the DC needs to be inverted back to AC for wireless transmission. In the DC to AC inverter (full-wave inverter) stage, the DC output from the rectifier is converted back into AC using a full-wave inverter. This high-frequency inverter plays a pivotal role in preparing the current for wireless transmission by generating the necessary alternating current. The transmission coil then receives this AC output, producing a magnetic field that is essential for WPT. The transmission coil's ability to generate a magnetic field allows for the efficient transfer of energy.

The process of wireless energy transfer occurs through inductive coupling. The energy is transmitted wirelessly from the transmission coil to the receiving coil through magnetic coupling, which is a key feature

of the WPT technology employed in this system. The receiving coil captures the AC energy transmitted wirelessly, acting as the counterpart to the transmission coil.

Once the AC energy is received, it is converted back to DC in the AC to DC rectification (high-frequency single-phase rectifier circuit) stage. This high-frequency single-phase rectifier circuit ensures that the AC captured by the receiving coil is converted into a usable DC form, suitable for powering various devices. Finally, the DC load receives the rectified DC power, completing the power supply process and delivering a steady and efficient power output to the end devices.

A detailed explanation of each circuit's design and function is provided in sections 2.1 and 2.2, offering comprehensive insights into the methodology and technical advancements achieved through this research. These sections delve into the intricate workings of the APF, the high-frequency inverter, and the WPT system. By thoroughly examining these components, the research highlights significant innovations in reducing harmonic distortions, improving power factor, and enhancing overall system efficiency, thereby setting new benchmarks in wireless DC power supply technology.
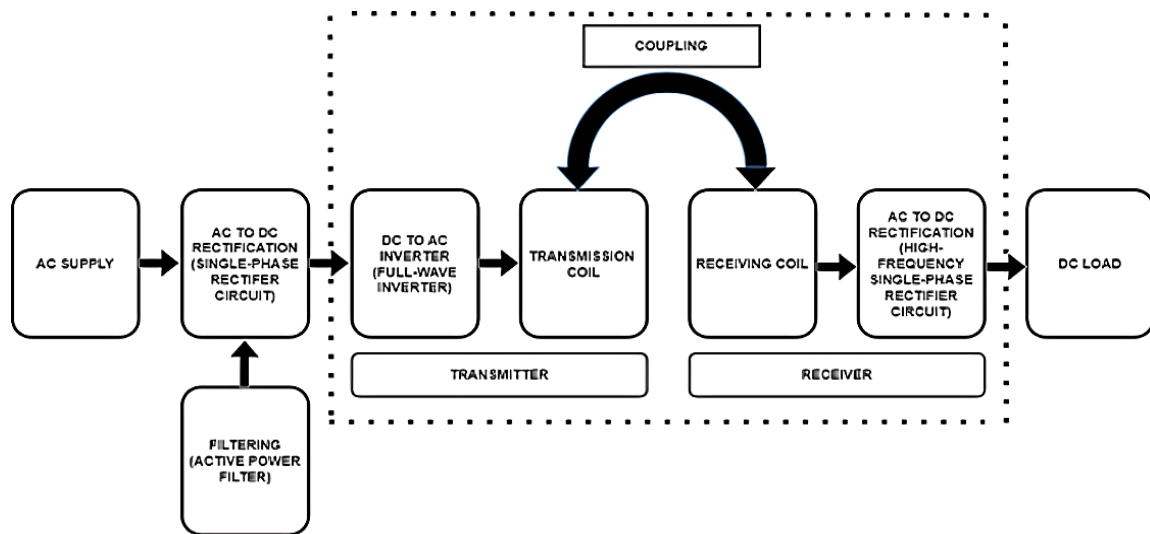

Figure 1. Block diagram of high power factor wireless DC power supply system

2.1. Rectifier with APF circuit

Figure 2 illustrates the integration of an APF into a single-phase rectifier circuit with a capacitive load. This detailed schematic showcases the interplay between various components that work together to improve the power quality and efficiency of the system. The circuit model consists of several key components: a diode bridge rectifier, a capacitive load, a single metal oxide semiconductor field effect transistor or MOSFET switch, and a current control loop (CCL). The diode bridge rectifier includes four diodes (D1, D2, D3, and D4), which convert AC supply into DC. The capacitive load is represented by Co and RL, which smooth out the pulsating DC output from the rectifier. The MOSFET switch (S1) is central to the APF operation, enabling dynamic control of the current flow.

Within the CCL, essential elements such as the reference current (Vref), subtractor, proportional-integral (PI) controller, carrier signal (Vcarrier 20 kHz), and comparator are incorporated. The AC supply current (Isense) is continuously monitored and processed by the CCL. The absolute value circuits (Abs1 and Abs2) convert the negative portions of the waveform to positive values, ensuring both the AC supply current and the reference AC current are in a comparable form. The subtractor then generates an error signal by comparing the actual AC supply current with the reference current.

This error signal is fed into the PI controller, which adjusts the response signal to enhance the dynamic response of the system. The output from the PI controller is then compared with a 20 kHz carrier signal in the comparator to produce the active pulse width modulation (APWM) switching signal. This APWM signal controls the MOSFET switch (S1), regulating the operation of the APF.

The APF circuit operates in four distinct modes to manage the AC current flow and improve power quality. In mode 1, during the positive half-cycle of the AC input, switch S1 is activated, allowing the AC supply current to flow through the line inductor (Ls), diode D1, the power switch S1, and exits via diode D2 to the negative supply. Mode 2 begins when S1 is deactivated, directing the current through Ls, D1, and D5

towards the RC loads, returning to the negative supply via D2. These modes charge Ls, increasing the line current during the positive half-cycle.

Modes 3 and 4 mirror the operations of modes 1 and 2 but occur during the negative half-cycle of the AC input. In mode 3, the AC current flows when S1 is engaged, channeling the current through D3, S1, and back to the positive AC supply terminal via D4. In mode 4, with S1 disengaged, Ls discharges, directing the energy to the resistive load, resulting in a diminishing input current waveform. This comprehensive cycle of operations ensures effective harmonic compensation and enhanced power quality within the circuit.

2.2. Integration of high power factor rectifier with wireless DC power supply system

Figure 3 illustrates the integration of a WPT circuit with an APF circuit, forming a comprehensive system for high power factor rectification and wireless DC power supply. The diagram presents the sequence of components and their interactions, enhancing the efficiency and power quality of the system. The APF circuit serves as the initial stage, responsible for filtering and improving the quality of the AC supply current. This circuit mitigates harmonic distortions and corrects the power factor before the current is further processed. The output of the APF is then fed into a set of MOSFET switches (S1, S2, S3, S4), which operate as an inverter.

The pulse generator controls the MOSFET switches, orchestrating the switching process to convert the DC output from the APF into a high-frequency AC waveform. During this operation, pairs of switches are activated simultaneously: S1 and S2 during the first half of the cycle, and S3 and S4 during the latter half. This switching pattern ensures the efficient conversion of the DC input into a consistent AC waveform.

The high-frequency AC generated by the MOSFET switches is then passed through the transmitter coil (C1), which, together with the receiver coil (C2), forms the core of the WPT system. The mutual inductance between these coils allows for the wireless transfer of power. The transmitter coil generates a magnetic field that inductively couples with the receiver coil, enabling the transfer of energy without physical connections.

Once the high-frequency AC is received by the receiver coil, it is converted back into DC through a high-frequency rectifier circuit. This rectifier circuit consists of four diodes (D1, D2, D3, D4) arranged in a bridge configuration. During the positive half-cycle of the AC waveform, diodes D1 and D2 conduct, allowing current to flow through the load (RLoad). Conversely, during the negative half-cycle, diodes D3 and D4 conduct, ensuring continuous DC output. The final stage of the system delivers the rectified DC power to the load (RLoad). This seamless conversion and transfer of power, facilitated by the integrated APF and WPT circuits, demonstrate the system's ability to maintain high power quality and efficiency.
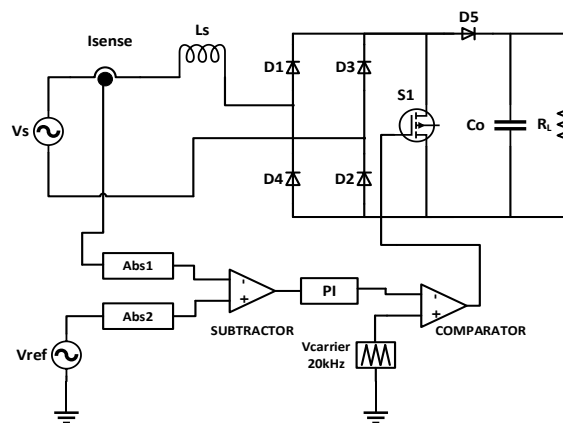

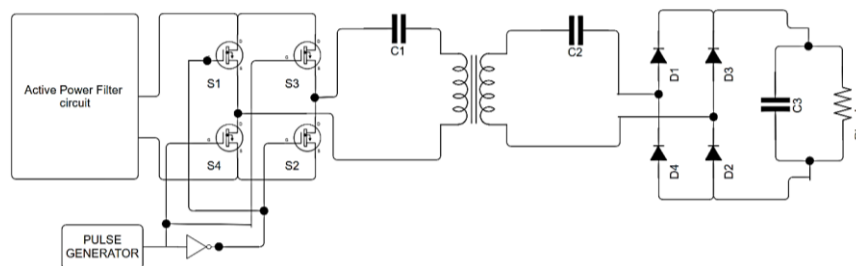Figure 2. Integration of rectifier with APF circuit

Figure 3. Integration of the WPT with the APF circuit

3.   COMPUTER SIMULATION MODEL

Figure 4 presents the computer simulation model of an APF circuit developed using MATLAB/Simulink while Table 1 shows parameter values for the components in the APF circuit. This detailed schematic highlights the configuration and functionality of the APF circuit, designed to improve power quality by reducing harmonic distortions and enhancing the power factor. The model incorporates a bridge rectifier configuration consisting of four diodes (D1, D2, D3, and D4). Each diode is paralleled by a series RC snubber circuit to protect against voltage spikes and ensure stable operation. The rectifier converts the AC supply voltage (Vs) into DC, which is then filtered by the capacitive load (Co) and the resistive load (RLoad). The RLC branches are arranged in parallel, with one branch containing the capacitor Co and the other the resistor RLoad. The resistance values for both the series RC snubber circuit and the RLoad are identical, set at 0.001 Ω and 500 Ω, respectively, while the snubber circuit's capacitance is 250 nF. Additional components introduced in this model include a MOSFET switch, diode D5, and a line inductor (Ls). The MOSFET switch plays a crucial role in the APF operation by dynamically regulating the current flow to correct the power factor and reduce harmonic distortions. Diode D5 helps in directing the current flow appropriately within the circuit.

The CCL is a vital part of the APF circuit, incorporating several essential elements. The reference signal is generated using a sine wave block from MATLAB/Simulink, ensuring that the desired waveform is continuously compared against the actual supply current. An absolute value block (ABS) is used to convert negative waveform values to positive, making it easier to process the signals.

The PI controller within the CCL is configured to regulate the error signal generated by subtracting the actual current from the reference current. The PI controller fine-tunes the response, improving the dynamic behavior of the system. The output of the PI controller is then fed into a comparator block, derived from a greater-than block, which compares it against a carrier signal of 20 kHz to generate the APWM signal. This APWM signal controls the MOSFET switch, enabling precise adjustments to the current flow. The simulation model also includes parameters for each component to provide a comprehensive overview of the circuit's configuration. For instance, the line inductor (Ls) is designed to smooth out the current and reduce ripple, enhancing the overall stability and performance of the circuit.
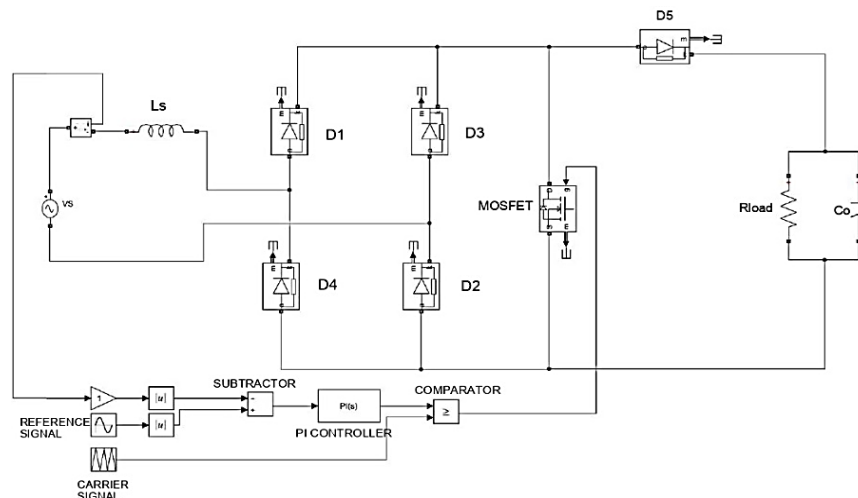

Figure 4. Computer simulation model of APF circuit using MATLAB/Simulink

Table 1. Parameter values for the components in the APF circuit

Components	Values
Voltage supply, Vs	Voltage = 40*sqrt(2) V
	Frequency = 50Hz
Diode D1-D5	Resistance = 0.001Ω
	Snubber resistance = 500 Ω
	Snubber capacitance = 250e-9 F
MOSFET	FET resistance = 0.1Ω
	Internal diode resistance = 0.01 Ω
	Snubber resistance = 1e5 Ω
Line inductor, Ls	Inductance = 0.5e-3 H
PI controller	Proportional gain, P = 320
	Integral gain, I = 1300

Figure 5 illustrates the computer simulation model of a high-power factor wireless DC power supply circuit, developed using MATLAB/Simulink. This comprehensive model integrates four distinct circuits: the APF circuit, a high-frequency inverter circuit, the WPT circuit, and a high-frequency rectifier circuit. The APF circuit block is the first stage of the system. It includes a bridge rectifier formed by four diodes (D1, D2, D3, and D4), which converts the AC supply into DC. This stage also incorporates a series inductor (Ls) that smooths the current and reduces ripples. The CCL within the APF circuit comprises essential components such as the reference signal generator, absolute value blocks (Abs1 and Abs2), a subtractor, a PI controller, and a comparator. These elements work together to generate a stable and clean DC output by dynamically regulating the current flow through a MOSFET switch.

Next, the high-frequency inverter circuit takes the DC output from the APF and converts it into a high-frequency AC signal. This circuit includes four MOSFET switches (S1, S2, S3, and S4), each equipped with an internal diode and connected in parallel. The switching of these MOSFETs is meticulously controlled by an APWM signal. This signal is generated using a combination of a repeating sequence block, a constant block, and a greater-than block within the inverter subsystem. The precise control provided by the APWM signal ensures efficient and effective conversion of the DC input into an AC waveform suitable for wireless transmission.

The WPT circuit is responsible for the wireless energy transfer between the transmitter and receiver coils. The transmitter coil (C1) generates a magnetic field when energized by the high-frequency AC signal from the inverter. This magnetic field induces a current in the receiver coil (C2) through mutual inductance, allowing for the wireless transfer of power. The WPT circuit effectively simulates the coupling between these coils, facilitating the efficient transmission of energy without physical connections.

Finally, the high-frequency rectifier circuit converts the high-frequency AC signal received by the WPT circuit back into DC. This circuit consists of another set of four diodes (D1, D2, D3, and D4) arranged in a bridge configuration. During the positive half-cycle of the AC waveform, diodes D1 and D2 conduct, while during the negative half-cycle, diodes D3 and D4 take over. This ensures a continuous and smooth DC output, which is further filtered by a capacitor (C3) to eliminate any remaining ripples, before being delivered to the load (RLoad). Table 2 presents the parameter values for the components in the WPT circuit.
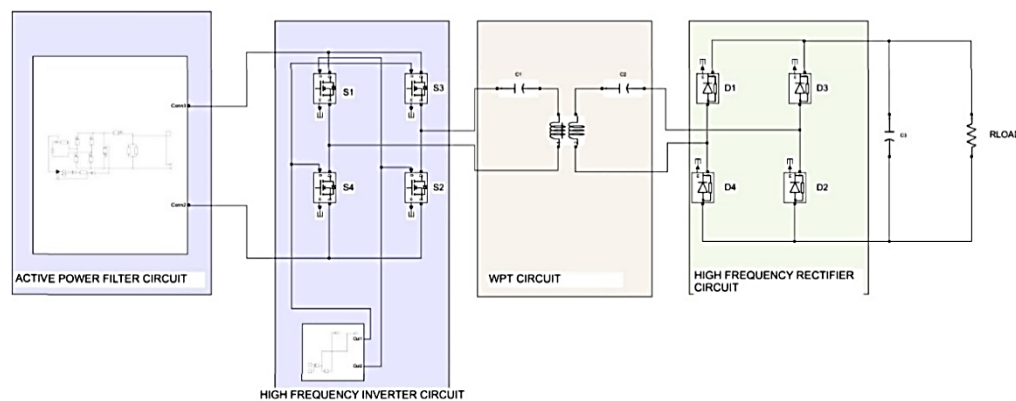

Figure 5. Simulation model of high-power factor wireless DC power supply circuit

Table 2. Parameter values for the components in the WPT circuit

Components	Values
MOSFET S1-S4	FET resistance = 0.1 Ω
	Internal diode resistance = 0.01 Ω
	Snubber resistance = 1e5 Ω
Capacitor C1 and C2	7e-6 F
Mutual Inductance	Winding 1 self-impedance = 0.082 Ω & 2.4e-5 H
	Winding 2 self-impedance = 0.082 Ω & 2.4e-5 H
	Mutual impedance = 1.0 Ω & 12e-6 H
Capacitor, Co	Capacitance = 20e-6 F
Resistor, Rload	11 Ω

4. RESULTS AND DISCUSSION

Figures 6 to 8 provide a comprehensive overview of the power quality issues in a system without an APF. Figure 6 illustrates the distorted supply current waveform, characterized by sharp spikes and dips, which result in a THD value of 261.07%. This high THD value, calculated using MATLAB/Simulink, involves

decomposing the current waveform into its harmonic components via fast Fourier transform (FFT) and calculating the root mean square (RMS) values of these components relative to the fundamental frequency as presented in (1).

$$THD = \frac{\sqrt{\sum_{n=2}^{\infty} I_n^2}}{I_1} \times 100\% \tag{1}$$

Where I_n is the RMS value of the nth harmonic component, and I_1 is the RMS value of the fundamental frequency. In MATLAB/Simulink, this can be achieved by using the 'power_analyze' function or the 'fft' function to perform the FFT and compute the THD.
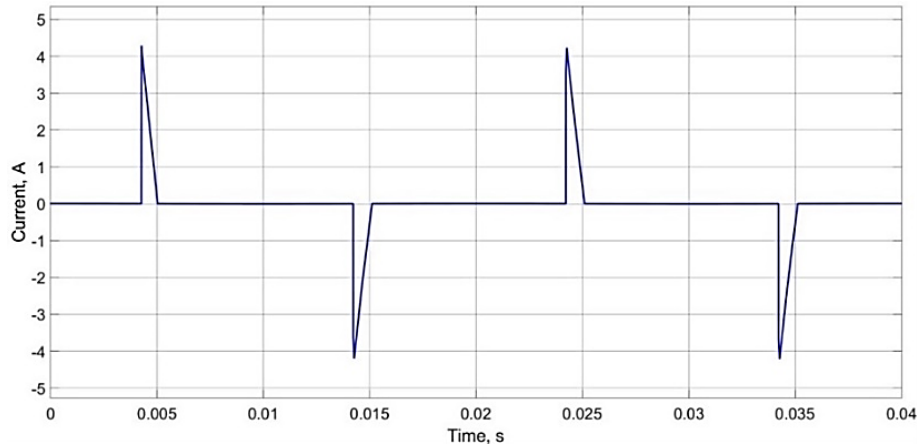
Figure 6. Distorted supply current waveform without APF function

Following this, Figure 7 presents the output voltage waveform of the system. The vertical axis represents the voltage in volts (V), while the horizontal axis represents time in seconds (s). The waveform exhibits periodic fluctuations, with voltage levels varying between approximately 52 volts and 56 volts.

Figure 8 compares the harmonic spectrum of the supply current without the APF to the IEEE 519 standard. The results show that the third harmonic is the most prominent, with a THD percentage of 98.26%, far exceeding the standard's allowable limit of 4%. Other harmonics, especially the 5th, 7th, 9th, and 11th, also show THD levels well above acceptable limits, highlighting severe power quality issues. The analysis of these figures underscores the critical need for implementing an APF in the system. High harmonic levels can cause equipment damage, efficiency losses, and operational interference, making it essential to dynamically compensate for these distortions.
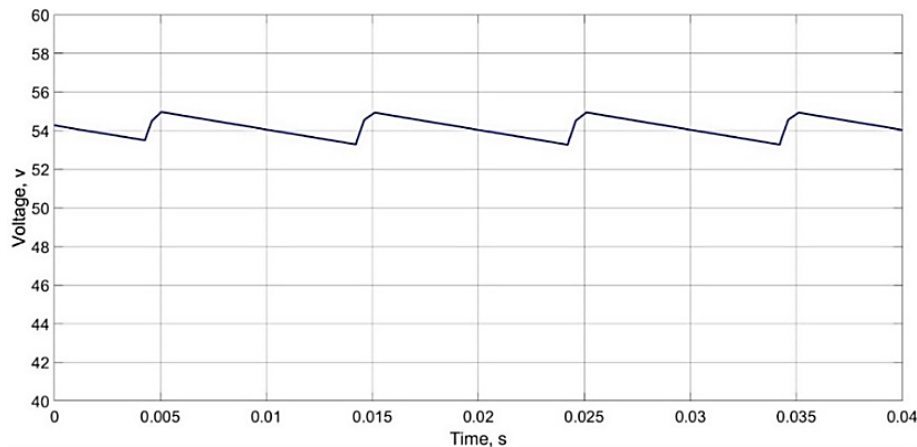

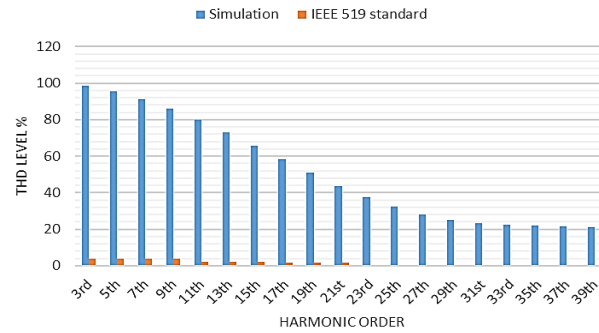Figure 7. Output voltage waveform

Figure 8. Comparison of harmonic spectrum of distorted supply current waveform with IEEE 519 standard

Figure 9 effectively demonstrates the efficacy of the APF in achieving successful harmonic compensation. The supply current waveform is shown as both sinusoidal and continuous, indicative of a well-compensated system. The waveform's smooth shape contrasts starkly with the distorted waveform seen without the APF, highlighting the significant improvement in power quality. The implementation of the APF has resulted in a dramatic decrease in THD to 1.70%, showcasing its capability to mitigate harmonics and enhance the overall efficiency of the electrical system.

Proceeding to Figure 10, it illustrates the waveforms of both the supply voltage and supply current after compensation. The waveforms are in phase and exhibit a continuous sinusoidal shape, indicating that the APF has successfully synchronized the current with the voltage. This alignment is crucial for improving the power factor and ensuring efficient power transfer. The visual representation confirms that the APF has effectively reduced the harmonic content, resulting in a cleaner and more stable current that closely follows the reference waveform.
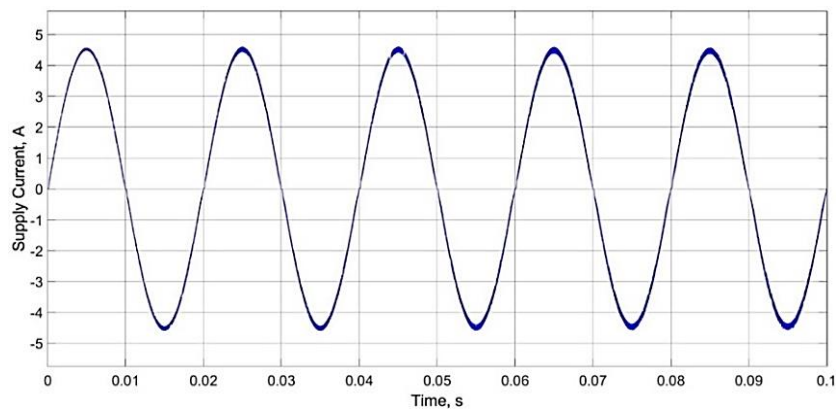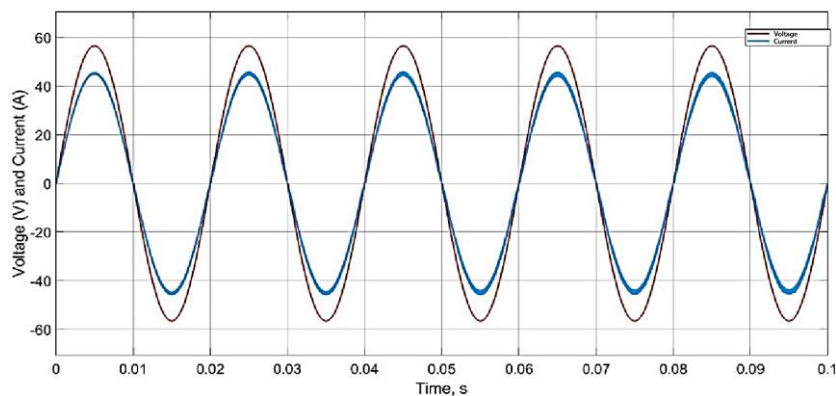

Figure 9. Supply current waveform with APF

Figure 10. Supply current and voltage waveforms with APF (ratio voltage: current=1:1/10)

Figure 11 further delineates the synchronization of the supply current waveform with the reference current waveform. The precise alignment between the two waveforms indicates the APF's ability to dynamically adjust and compensate for distortions in real-time. This synchronization ensures that the supply current adheres closely to the desired reference current, minimizing deviations and enhancing power quality. The APF's control mechanisms, including current sensing, error signal processing, and compensating current injection, work in harmony to achieve this precise alignment.
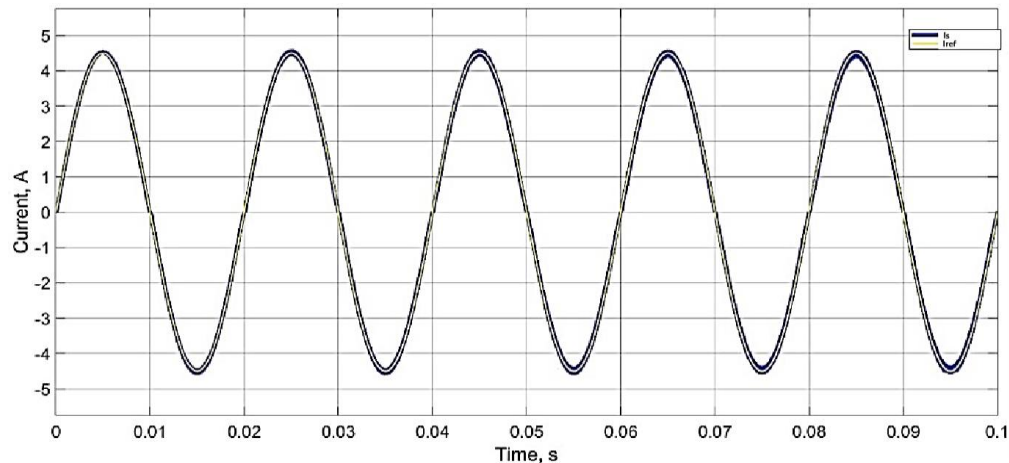

Figure 11. AC supply current (Is) follows the reference current (Iref) waveform

Lastly, Figure 12 reveals the harmonic spectrum of the compensated system, illustrating a notable reduction in harmonic components. The third harmonic's percentage has been significantly reduced to 0.76%, well within the IEEE 519 standard's maximum allowable threshold of 4%. This figure also displays considerable reductions in the percentages of the remaining harmonic components, further underscoring the comprehensive effectiveness of the APF in enhancing power quality. The comparison between the simulation results and the IEEE 519 standards demonstrates that the THD levels for all harmonic orders are substantially lower than the allowable limits, ensuring compliance, and optimal performance.

Figure 13 illustrates the voltage waveform at the transmitter coil of the WPT system. The vertical axis represents voltage in volts (V), while the horizontal axis represents time in seconds (s). The waveform shows high-frequency oscillations centered around zero volts, indicative of a high-frequency AC signal. This high-frequency signal is essential for efficient energy transfer between the transmitter and receiver coils. The waveform's symmetry around the zero voltage line indicates balanced AC voltage, which is crucial for creating a stable magnetic field necessary for effective wireless energy transfer.
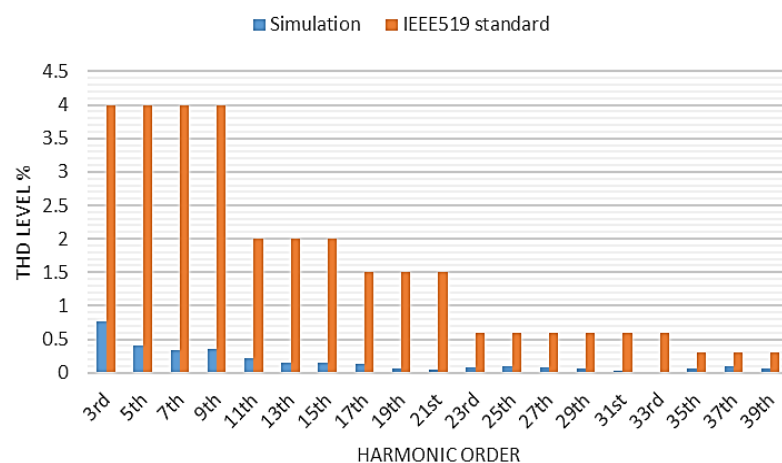

Figure 12. Comparison of harmonic spectrum of sinusoidal supply current waveform in accordance with IEEE 519 standard
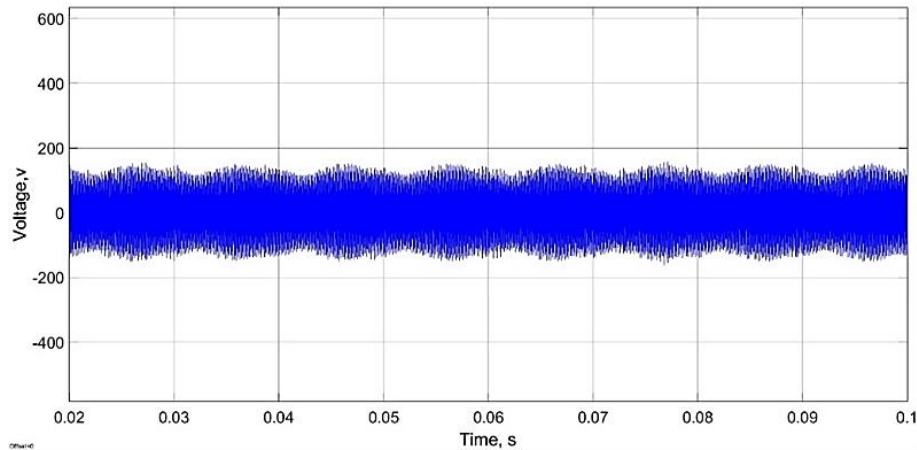
Figure 13. Voltage waveform at transmitter coil of WPT

Figure 14 presents the voltage waveform at the receiver coil of the WPT system. Similar to the transmitter coil, the vertical axis represents voltage in volts (V), and the horizontal axis represents time in seconds (s). The waveform shows high-frequency oscillations, but these are slightly attenuated compared to the transmitter coil's voltage. The symmetrical oscillations around zero volts confirm that the receiver coil effectively converts the transmitted magnetic field back into an electrical signal. The high-frequency nature of the signal ensures efficient energy transfer and minimal energy loss, which is essential for the system's overall performance.

Figure 15 illustrates the output voltage waveform of the WPT system after rectification and filtering. The vertical axis represents voltage in volts (V), and the horizontal axis represents time in seconds (s). The output voltage fluctuates around an average value of approximately 80 volts, with peak values reaching up to 100 volts. The presence of periodic ripples in the waveform indicates that the rectification process has introduced some AC components into the DC voltage. These ripples are typical in rectified voltages and highlight the need for effective filtering to achieve a stable DC output. The relatively narrow band of fluctuations suggests a degree of stability, which is essential for the reliable operation of connected load devices.

The analysis of Figures 13 to 15 underscores the critical stages of voltage transformation in a WPT system. Figure 13 demonstrates the generation of a high-frequency AC voltage at the transmitter coil, essential for creating a magnetic field for wireless energy transfer. Figure 14 shows the successful reception and conversion of this magnetic field into a high-frequency electrical signal at the receiver coil. The high-frequency operation in both figures is vital for efficient energy transfer and reducing energy losses.

Figure 15 highlights the final stage of voltage transformation, where the high-frequency AC signal is rectified and filtered to provide a DC output to the load. The average voltage level of 80 volts is suitable for the load, but the presence of voltage ripples indicates the need for improved filtering. Effective filtering would minimize these ripples, resulting in a more stable DC output, enhancing the performance and lifespan of the connected devices.
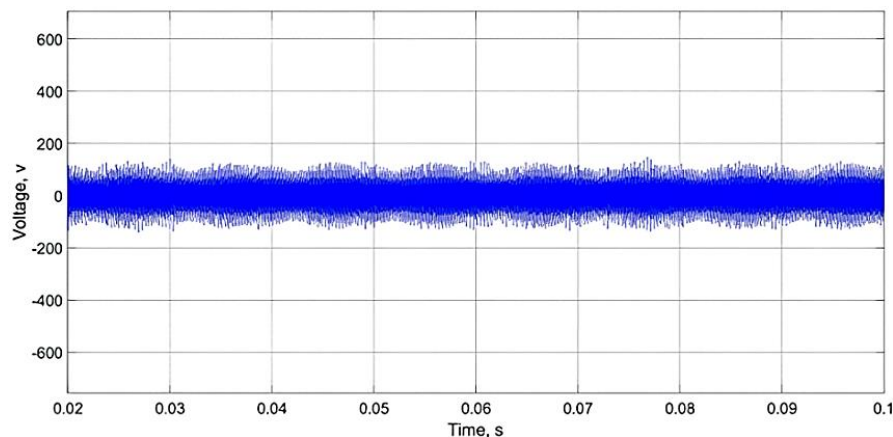

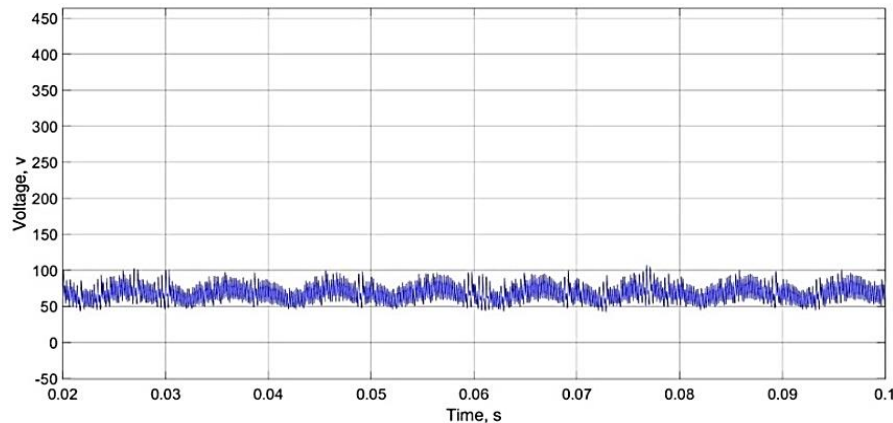Figure 14. Voltage waveform at receiver coil of WPT

Figure 15. Output voltage of the WPT system

5. CONCLUSION

This paper presents a detailed analysis and simulation of a high-power factor wireless DC power supply system integrating APF and WPT technology. The results demonstrate significant improvements in power quality through these advanced techniques. The APF effectively reduces THD to 1.70%, creating a smooth, sinusoidal supply current waveform. This improvement highlights the APF's capability to mitigate harmonics and enhance system efficiency. Additionally, post-compensation synchronization of supply voltage and current waveforms confirms the APF's role in improving power factor and ensuring efficient power transfer. The harmonic spectrum analysis reveals substantial reductions in harmonic components, with the third harmonic reduced to 0.76%, meeting the IEEE 519 standard. This compliance underscores the APF's effectiveness in enhancing power quality and maintaining industry standards.

Voltage transformation stages in the WPT system show efficient high-frequency energy transfer between the transmitter and receiver coils. In conclusion, integrating APF and WPT technologies in a high-power factor wireless DC power supply system significantly enhances power quality, system efficiency, and compliance with industry standards. These technologies are vital for modern electrical systems, ensuring reliable and efficient power delivery across various applications. Future research should focus on optimizing filtering processes to further stabilize the output voltage, enhancing performance and reliability for connected devices. Additionally, exploring advanced materials and designs for coils and filters could further improve the efficiency and effectiveness of WPT systems.

REFERENCES

[1]   Q. Li, X. Tang, X. Shi, H. Liu, Z. Li, and J. Yan, "Demonstration and application of AC/DC hybrid power supply system in building," in *2018 2nd IEEE Conference on Energy Internet and Energy System Integration (EI2)*, IEEE, Oct. 2018, pp. 1–6. doi: 10.1109/EI2.2018.8582268.

[2]   R. Baharom, M. Z. Rosman, I. Yassin, and N. F. Abdul Rahman, "Development of single-phase active power filter using current source inverter (CSI)," in *2019 IEEE 9th Symposium on Computer Applications & Industrial Electronics (ISCAIE)*, IEEE, Apr. 2019, pp. 64–68. doi: 10.1109/ISCAIE.2019.8743834.

[3]   R. Baharom, N. Ahman, and N. F. A. Rahman, "Development of single-phase active power filter using voltage source inverter (VSI)," in *2019 IEEE 9th Symposium on Computer Applications & Industrial Electronics (ISCAIE)*, IEEE, Apr. 2019, pp. 60–63. doi: 10.1109/ISCAIE.2019.8743840.

[4]   M. Xiao, Y. Zhu, L. Meng, K. Lu, and Z. Wu, "Current harmonic suppression for high-speed air compressor based on improved discrete-time current controller and LC filter," in *2022 IEEE Vehicle Power and Propulsion Conference (VPPC)*, IEEE, Nov. 2022, pp. 1–7. doi: 10.1109/VPPC55846.2022.10003316.

[5]   K. Okawa, K. Murakami, K. Fukushima, and N. Okada, "Measurement-based harmonic current modeling of agricultural heat pumps," in *2022 IEEE PES 14th Asia-Pacific Power and Energy Engineering Conference (APPEEC)*, IEEE, Nov. 2022, pp. 1–6. doi: 10.1109/APPEEC53445.2022.10072175.

[6]   N.-T. Trinh and F. Vidal-Naquet, "Current harmonic suppression for permanent magnet synchronous motors," in *2019 International Aegean Conference on Electrical Machines and Power Electronics (ACEMP) & 2019 International Conference on Optimization of Electrical and Electronic Equipment (OPTIM)*, IEEE, Aug. 2019, pp. 161–165. doi: 10.1109/ACEMP-OPTIM44294.2019.9007209.

[7]   R. Baharom, M. K. M. Salleh, and N. F. A. Rahman, "Active power filter with direct output voltage control of single-phase AC to DC converter," in *2016 IEEE International Conference on Power and Energy (PECon)*, IEEE, Nov. 2016, pp. 412–416. doi: 10.1109/PECON.2016.7951597.

[8] J. Liu, F. Xu, C. Sun, and K. H. Loo, "A compact single-phase AC–DC wireless power transfer converter with active power factor correction," *IEEE Transactions on Industrial Electronics*, vol. 70, no. 4, pp. 3685–3696, Apr. 2023, doi: 10.1109/TIE.2022.3176297.

[9] S. Rahmani, A. Hamadi, K. Al-Haddad, and L. A. Dessaint, "A combination of shunt hybrid power filter and thyristor-controlled reactor for power quality," *IEEE Transactions on Industrial Electronics*, vol. 61, no. 5, pp. 2152–2164, May 2014, doi: 10.1109/TIE.2013.2272271.

[10] X. Mou and H. Sun, "Wireless power transfer: survey and roadmap," in *2015 IEEE 81st Vehicular Technology Conference (VTC Spring)*, IEEE, May 2015, pp. 1–5. doi: 10.1109/VTCSpring.2015.7146165.

[11] Z. Zhang, H. Pang, A. Georgiadis, and C. Cecati, "Wireless power transfer-An overview," *IEEE Transactions on Industrial Electronics*, vol. 66, no. 2, pp. 1044–1058, Feb. 2019, doi: 10.1109/TIE.2018.2835378.

[12] J. Huang, Y. Zhou, Z. Ning, and H. Gharavi, "Wireless power transfer and energy harvesting: current status and future prospects," *IEEE Wirel Commun*, vol. 26, no. 4, pp. 163–169, Aug. 2019, doi: 10.1109/MWC.2019.1800378.

[13] J. Shin, S. Shin, Y. Kim, S. Lee, B. Song, and G. Jung, "Optimal current control of a wireless power transfer system for high power efficiency," in *2012 Electrical Systems for Aircraft, Railway and Ship Propulsion*, IEEE, Oct. 2012, pp. 1–4. doi: 10.1109/ESARS.2012.6387426.

[14] Z. Yan *et al.*, "Efficiency improvement of wireless power transfer based on multitransmitter system," *IEEE Trans Power Electron*, vol. 35, no. 9, pp. 9011–9023, Sep. 2020, doi: 10.1109/TPEL.2020.2971140.

[15] F. Liu, K. Chen, Z. Zhao, K. Li, and L. Yuan, "Transmitter-side control of both the CC and CV modes for the wireless EV charging system with the weak communication," *IEEE Journal of Emerging and Selected Topics in Power Electronics*, vol. 6, no. 2, pp. 955–965, Jun. 2018, doi: 10.1109/JESTPE.2017.2759581.

[16] S. Shin *et al.*, "Wireless power transfer system for high power application and a method of segmentation," in *2013 IEEE Wireless Power Transfer (WPT)*, IEEE, May 2013, pp. 76–78. doi: 10.1109/WPT.2013.6556886.

[17] H. Le-Huu, N. Ha-Van, S. Hong, and C. Seo, "Multiple-receiver wireless power transfer system using a cubic transmitter," in *2019 IEEE Wireless Power Transfer Conference (WPTC)*, IEEE, Jun. 2019, pp. 170–173. doi: 10.1109/WPTC45513.2019.9055603.

[18] H. Allamehzadeh, "Wireless power transfer (WPT) fundamentals with resonant frequency-dependent parameters, energy transfer efficiency, and green technology applications," in *2021 IEEE 48th Photovoltaic Specialists Conference (PVSC)*, IEEE, Jun. 2021, pp. 0036–0040. doi: 10.1109/PVSC43889.2021.9518505.

[19] J. Choi, D. Tsukiyama, Y. Tsuruda, and J. M. R. Davila, "High-frequency, high-power resonant inverter with eGaN FET for wireless power transfer," *IEEE Trans Power Electron*, vol. 33, no. 3, pp. 1890–1896, Mar. 2018, doi: 10.1109/TPEL.2017.2740293.

[20] S. Ansari, A. Das, and A. Bhattacharya, "Resonant inductive wireless power transfer of two-coil system with class-E resonant high frequency inverter," in *2019 6th International Conference on Signal Processing and Integrated Networks (SPIN)*, IEEE, Mar. 2019, pp. 269–273. doi: 10.1109/SPIN.2019.8711782.

[21] J. Liu, W. Xu, K. W. Chan, M. Liu, X. Zhang, and N. H. L. Chan, "A three-phase single-stage AC–DC wireless-power-transfer converter with power factor correction and bus voltage control," *IEEE Journal of Emerging and Selected Topics in Power Electronics*, vol. 8, no. 2, pp. 1782–1800, Jun. 2020, doi: 10.1109/JESTPE.2019.2916258.

[22] A. Puzakov and A. Arhirejskij, "Mathematical model of operability of a single-phase bridge rectifier," in *2022 8th International Conference on Energy Efficiency and Agricultural Engineering (EE&AE)*, IEEE, Jun. 2022, pp. 1–5. doi: 10.1109/EEAE53789.2022.9831215.

[23] H. Y. Gangadhara and K. Deepa, "Dynamic wireless power transfer using an isolated DC-DC converter," in *2022 Trends in Electrical, Electronics, Computer Engineering Conference (TEECCON)*, IEEE, May 2022, pp. 7–13. doi: 10.1109/TEECCON54414.2022.9854514.

[24] Z. Liu, H. Zhang, P. Han, and X. He, "Research on secondary ripple suppression of single-phase rectifier based on CRH3," in *2021 IEEE International Conference on Predictive Control of Electrical Drives and Power Electronics (PRECEDE)*, IEEE, Nov. 2021, pp. 296–299. doi: 10.1109/PRECEDE51386.2021.9680972.

[25] Md. A. Yousuf, T. K. Das, Md. E. Khallil, N. A. Ab. Aziz, Md. J. Rana, and S. Hossain, "Comparison study of inductive coupling and magnetic resonant coupling method for wireless power transmission of electric vehicles," in *2021 2nd International Conference on Robotics, Electrical and Signal Processing Techniques (ICREST)*, IEEE, Jan. 2021, pp. 737–741. doi: 10.1109/ICREST51555.2021.9331096.

[26] S. M. Halpin, "Comparison of IEEE and IEC harmonic standards," in *2005 IEEE Power Engineering Society General Meeting*, IEEE, 2005, pp. 2214–2216. doi: 10.1109/pes.2005.1489688.

BIOGRAPHIES OF AUTHORS

Rahimi Baharom ⬛ 🆂🅲 ⬛ is a lecturer in School of Electrical Engineering, College of Engineering, Universiti Teknologi MARA, Malaysia since 2009; and He has been a senior lecturer since 2014. He received the B.Eng. degree in Electrical Engineering and the M.Eng. degree in Power Electronics, both from Universiti Teknologi MARA, Malaysia, in 2003 and 2008, respectively; and Ph.D. degree in Power Electronics also from Universiti Teknologi MARA, Malaysia in 2018. He is a senior member of IEEE and also a corporate member of the Board of Engineers Malaysia and the member of Malaysia Board of Technologists. His research interests include the field of power electronics, motor drives, industrial applications, and industrial electronics. He can be contacted at email: rahimi6579@gmail.com.

Wan Muhamad Hakimi Wan Bunyamin ⬛ 🆂🅲 ⬛ is a postgraduate student in School of Electrical Engineering, College of Engineering, Universiti Teknologi MARA, Malaysia since 2022. He received the B.Eng. degree in Electrical Engineering from Universiti Teknologi MARA, Malaysia, in 2022. He is a student member of IEEE, a graduate engineer of Board of Engineers Malaysia and a graduate technologist of Malaysia Board of Technologists. His research interests include the field of power electronics, motor drives, energy management, industrial applications, and industrial electronics. He can be contacted at email: wmhakimi11@gmail.com.